Effect of Solvent on Properties of Solution-Cast Dense SPPO Films

B. Kruczek, T. Matsuura

Department of Chemical Engineering, University of Ottawa, 161 Louis Pasteur Street, P. O. Box 450, Stn. A, Ottawa, Ontario K1N 6N5, Canada

Received 23 October 2001; accepted 13 September 2002
Published online 18 February 2003 in Wiley InterScience (www.interscience.wiley.com). DOI 10.1002/app.12032

ABSTRACT: The effect of solvent on properties of solution-cast dense films was investigated using high molecular weight sulfonated poly(2,6-dimethyl-1,4-phenylene oxide) (SPPO) and five different solvents having relatively similar molar volumes. The study revealed that polymer–solvent interactions existing in casting solution primarily determine the concentration of residual solvent and surface morphology of the films. On the other hand, the O_2 and CO_2 permeabilities, which for most permeable films were more than three times greater than for the least permeable ones, appear to be governed by the volatility of solvent in casting solution. At the same time, the more permeable films showed lower O_2/N_2 and CO_2/CH_4 permeability ratios than the less permeable ones. In addition to physical factors such as polymer–solvent interactions and volatility of solvent in casting solution, the differences in gas transport properties of SPPO films could arise from the formation of quaternary salts—in particular, in the case of films prepared from the pyridine solution. The analysis of casting solution properties, surface images by atomic force microscopy, and gas transport properties allowed us to associate defective structures of some SPPO films with a specific surface morphology and a particular combination of solvent properties. © 2003 Wiley Periodicals, Inc. J Appl Polym Sci 88: 1100–1110, 2003

Key words: sulfonated polyphenylene oxide; polymeric films; surface morphology; atomic force microscopy; gas permeability

INTRODUCTION

Poly(2,6-dimethyl-1,4-phenylene oxide) (SPPO) is a promising material for the preparation of gas separation membranes.[1–8] Our experience with this polymer shows that depending on the solvent, solution-cast dense SPPO films exhibit significant variation in gas transport properties. On the other hand, for a given combination of the degree of sulfonation (DS) and solvent, the gas transport properties of SPPO films are repeatable.[7] Moreover, SPPO films showed good stability in more than two-month permeation tests with CO_2 at ambient temperature.[6,7]

The influence of solvent on properties of solution-cast dense films is not a new observation; it was reported previously by a number of researchers.[9–17] The nature of solvent in casting solution is believed to affect conformation, size, and asymmetry of the polymer coil in dry films.[5] However, our knowledge on how the properties of solution-cast dense films are affected and by which particular property or combination of properties of solvent is rather limited. Moreover, it can be argued that what is known as the solvent effect could simply be a result of the presence of residual solvent in polymeric films. This is because the complete removal of residual solvent can only be ensured by annealing the polymer above its glass transition temperature (T_g).[18–20]

In the case of SPPO annealing above T_g (>212°C) is not possible without altering the chemistry of polymer. This is because sulfonic groups start to decompose at around 170°C.[8,21] Consequently, the presence of residual solvent in SPPO films, even in those extensively dried at an ultrahigh vacuum and ambient temperature, is quite possible. Whether or not the variation in gas transport properties of SPPO results from the nature of solvent in casting solution or from the presence of residual solvent, it is important to systematically quantify effect of solvent. Perhaps we will be able to take advantage of this knowledge in the design of gas separation membranes. Moreover, even if the presence of residual solvent is entirely responsible for the variation in gas transport properties, the question arises on how the amount of residual solvent depends on the properties of solvent in a casting solution under a given drying protocol.

In this article, the properties of solution-cast dense films prepared from solutions of high molecular weight SPPO of DS equal to 18.5% in different solvents are reported. The solvents are characterized by their molecular size, strength, and volatility, while the films

Correspondence to: B. Kruczek (kruczek@eng.uottawa.ca).
Contract grant sponsor: Natural Sciences and Engineering Research Council of Canada.
Contract grant sponsor: British (Consumers) Gas.

are characterized by spectra from thermogravimetric analysis, surface images by atomic force microscope (AFM), and gas transport properties. Using the above experimental data, we attempted to qualitatively distinguish between the effect of solvent properties and the effect of presence of residual solvent, and thus to correlate surface morphology and gas transport properties with the properties of solvents.

EXPERIMENTAL

Materials

Poly(2,6-dimethyl-1,4-phenylene oxide) (PPO) of intrinsic viscosity equal to 1.8 dL/g in chloroform at 25°C and silicone rubber membranes were purchased from General Electric. Sulfonation of PPO was carried out in chloroform solvent using chlorosulfonic acid as a sulfonating agent.[22,23] The extent of sulfonation was controlled by the amount of chlorosulfonic acid added. The degree of sulfonation, which is the average number of sulfonic groups per repeat unit of the polymer, was maintained at 18.5%. The details of the sulfonation procedure and the determination of DS of SPPO are described elsewhere.[6,7]

Chloroform of analytical grade stabilized with hydrocarbons, which was used in sulfonation reaction, and 0.1 N sodium hydroxide standard, which was used for the determination of DS of SPPO, were purchased from BDH. Other solvents and chemicals of analytical or reagent grade were purchased from the Aldrich Chemicals.

Preparation of dense films

Table I shows the list of solvents considered for dissolution of the polymer along with their solubility parameters.[24] Out of the 10 solvents considered, only 5 could dissolve the polymer. All casting solutions were prepared to the same concentration of 4 g /100 mL. Approximately 4 mL of casting solution was poured inside a 9 cm diameter metal ring placed onto a leveled glass plate, and the ring was then covered by a filter paper. With the exception of THF solution, which was cast at ambient temperature, all films were cast in a forced convection oven at 40 or 60°C. The solvent was allowed to evaporate for two days, after which the plate was put into a distilled water to facilitate the removal of the film from the plate.

Film drying was a multistage process. The freestanding films were first air dried at ambient temperature for one day, followed by air drying at 60°C for another day. The films were then dried in vacuum at pressure less than 1 cm Hg (absolute) and ambient temperature for at least two days. The final film-drying step took place in a testing cell at 0.0003 cm Hg (absolute) and ambient temperature for at least one day.

TABLE I
Hansen and Hildebrand Solubility Parameters[a] for Selected Organic Solvents[24]

Solvent	δ_d ($MPa^{1/2}$)	δ_P ($MPa^{1/2}$)	δ_h ($MPa^{1/2}$)	δ ($MPa^{1/2}$)
Acetone	15.5	10.4	7.0	20.3
Chloroform	17.8	3.1	5.7	19.0
DMAC	16.8	11.5	10.2	22.1
DMF	17.4	13.7	11.3	24.8
Methanol	15.1	12.3	22.3	29.7
Nitroethane	16.2	12.1	4.1	22.7
NMP	18.0	12.3	7.2	23.1
Pyridine	19.0	8.8	5.9	21.9
TCE[b]	18.0	3.1	5.3	18.8
THF	16.8	5.7	8.0	18.6

δ_d: dispersion force component of Hansen solubility parameter; δ_P: dipole component of Hansen solubility parameter; δ_h: hydrogen-bonding component of Hansen solubility parameter; δ: Hildebrand solubility parameter.

[a] For SPPO of DS = 18.5, the Hansen solubility parameters are δ_d = 17.75, δ_P = 16.48, δ_h = 8.14, while the Hildebrand solubility parameter is δ = 25.54. All solubility parameters are in $MPa^{1/2}$.

[b] Trichloroethylene.

Viscosity measurements

Kinematic viscosities of pure solvents and the actual polymer solutions used for casting films were determined using Cannon–Fenske viscometers at 25°C. The efflux times of casting solutions were measured in the viscometer with capillary of size 150, while the efflux times of pure solvents were measured in the viscometer with capillary of size 50. The kinematic viscosity was then determined as the product of the capillary constant and the efflux time. Since the density of polymer solution was not significantly different from the density of pure solvent, the relative viscosity (η_{rel}) was calculated as the ratio of the kinematic viscosity of casting solution and that of pure solvent.

Gas permeation tests

Single gas permeation tests with N_2, O_2, CH_4, and CO_2 were performed in an automated constant volume testing system, which was described elsewhere.[6,7,25] The tests were performed at the upstream pressure of 500 cm Hg, while the downstream pressure varied from 0.001 to 1 cm Hg. When the downstream pressure reached 1 cm Hg (end of a cycle), the downstream volume was connected to a vacuum pump until the pressure dropped below 0.001 cm Hg. Permeation tests were carried out over at least several cycles until the average permeation in several consecutive cycles

reached a constant value. Permeability (in Barrer) of a film was calculated from

$$P = \frac{Ql}{A\Delta p}10^{10} \quad (1)$$

where Q is a steady state permeation rate in mL-(STP)/s, l is a film thickness (cm), A is a permeation area of the film (cm^2), and Δp(cm Hg) is a pressure difference across the membrane. The permeation area of the cells was 10.2 cm^2, and the gas permeation tests were carried out at ambient temperature (23–24°C). The thickness of a film was determined by calculating the average from at least 10 thickness readings taken by a micrometer from the entire permeation area of the tested film.

In case of defective films, they were laminated with a silicone rubber membrane and their permeability was evaluated from the following equation[26]:

$$P_2 = \frac{l_2 P_1 Q}{P_1 A\Delta p - Q l_1} \quad (2)$$

Subscripts 1 and 2 in eq. (2) refer to silicone rubber* and defective films, respectively, while Q is a steady state permeation rate through the laminated film.

Thermal analysis

Thermal stability of SPPO was examined using films previously tested for gas permeation, in a Seiko 220TG/DTA analyzer run from 25 to 600°C heated at 10°C/min. Tests were done in nitrogen flushed at 200 cm^3/min.

Microscopic analysis

The surface morphology of SPPO films was investigated using a Nanoscope III atomic force microscope (AFM), operating in the tapping mode (TM). The AFM equipment was purchased from the Digital Instruments, Santa Barbara, CA.

Before obtaining surface images, the calibration of the microscope was examined. The distances in X and Y directions (horizontal plane) measured on a 1 μm gold calibration grating differed less than 2%, while the distance in Z (vertical) direction measured on a 180 nm step height calibration standard differed less than 10% from the values provided by the manufacturer. The images were obtained using etched silicon probes having tip diameter ranging from 5 to 10 μm and half cone angle of 17° ± 2°.

Small squares of the edge ranging from 0.5 to 1 cm were cut from the films previously tested for gas permeation, and the squares were glued on metal disks. For each film, at least two samples were prepared, and at least two surface images in different sections of the sample were obtained. The surfaces were first imaged in a large scan size (12 × 12 μm) followed by a gradual zooming in a uniform section of the first image. The smallest scan size considered was 0.75 × 0.75 μm.

The surfaces were compared in terms of two of roughness parameters, the mean roughness, in nm (R_a), which is a mean value of the surface (Z data) relative to the center plane,† and the root mean square of the Z data, in nm (R_q), which is a standard deviation from Z values within a given area. The roughness parameters were calculated using image analysis software supplied with the AFM equipment.[27] The roughness parameters depend on the curvature and size of the sensing probe, as well as on the treatment of the captured surface data (planefitting, flattening, filtering, etc.). The comparison of the roughness data obtained in this study with literature data might therefore not be appropriate. All the surface images, however, which will be discussed here, were obtained using the same type of the scanning probes and following the same protocol for the image treatment.

The dimensions of features observed on images were estimated from cross-sectional profiles of the data along the reference line. An example of the measurement of surface features is shown in Figure 1. For each pair of cursors, the horizontal and vertical distances as well as the angle between the cursors are given in the right window. The reference line can be placed anywhere on the image. The cursors can be placed anywhere on the reference line.

RESULTS AND DISCUSSION

Properties of casting solution

Kesting and Fritzsche[28] listed factors that, apart from polymer type, purity, and molecular weight, may influence the structure and function of thin, dense solution-cast polymeric films. These factors include solvent strength, volatility and molecular size, concentration of polymer solution, concentration of residual solvent, environmental temperature, solution temperature, relative humidity, airflow rate, and nature of the casting surface. All films considered in this study were prepared from polymer solutions of the same concentration and temperature using the same casting surface. Moreover, environmental temperature, relative humidity, and airflow were all similar for *N,N*-dimethylformamide (DMF),*N,N*-dimethylacetamide (DMAC), and 1-methyl-2-pyrrolidinone (NMP) films. On the other hand, the parameters such as solvent strength,

*Permeability coefficients, in Barrer, for silicone rubber: $P(N_2) = 25$, $P(O_2) = 50$, $P(CH_4) = 80$, $P(CO_2) = 270$.

†The planes for which the volume enclosed in the image above and below this plane are equal.

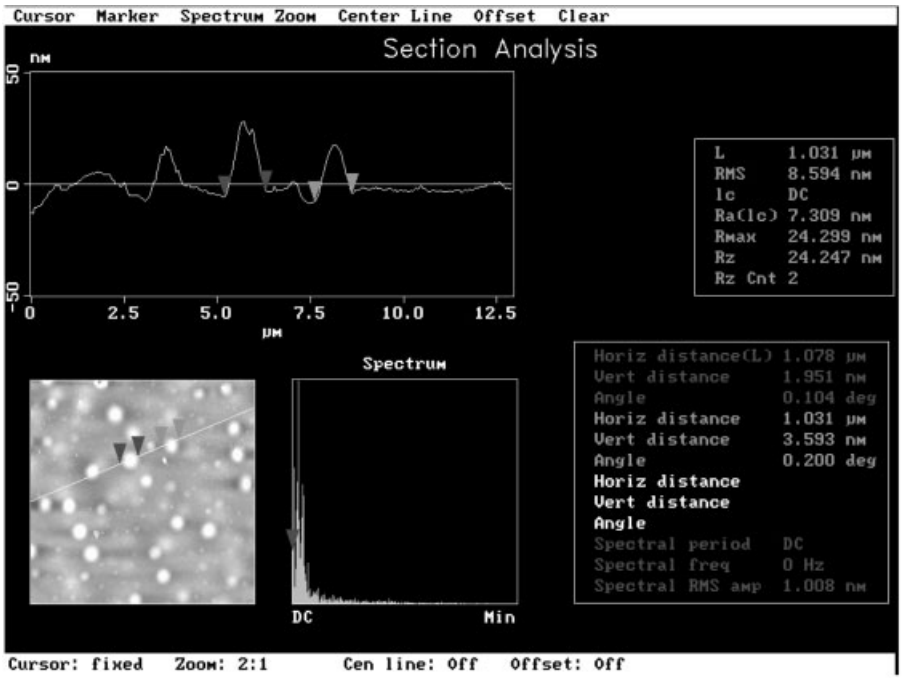

Figure 1 Example of measurement of features on film surface using AFM image software.

volatility and molecular size of solvent, and perhaps concentration of residual solvent, inevitably change with solvent in casting solution. Consequently, in order to understand the effect of solvent, the latter parameters should first be evaluated for all systems considered in this study.

Evaluation of solvent strength

Equilibrium configuration of molecular chains in polymer solution depends on the balance between the Gibbs free energy change due to mixing and that due to elastic deformation.[29] In dilute polymer solutions the extent of deformation of polymer chains depends on the relative strengths of polymer–polymer and polymer–solvent interactions. In a good (strong) solvent the polymer is unfolded, obtaining to the maximum extent the more favorable polymer–solvent interactions. On the other hand, in a poor solvent the polymer molecules remain folded because of more favorable polymer–polymer interactions. Consequently, the viscosity of a dilute solution of polymer reaches the maximum in strong solvents.

As the concentration of polymer increases, there is a "changeover" in behavior: the viscosity at higher concentrations becomes greater in poor than in strong solvents.[29–31] According to Kesting,[32] macromolecular aggregates exit in all but the most dilute polymer solutions. Their presence is a consequence of interaction between macromolecules in a crowded environment of polymer solution.[28] For a given concentration the tendency to form macromolecular aggregates should be enhanced by strong polymer–polymer and weak polymer–solvent interactions. Considering that the flow of polymer solution involves sliding of individual macromolecules upon one another, and that such sliding is resisted more within macromolecular aggregates than in a solution consisting of individual macromolecules, the minimum viscosity in strong solvents is not surprising. This qualitative consideration has been supported quantitatively by the data provided by Hoernschemeyer,[33] who showed that the viscosity of moderately concentrated polymer solution decreases with a decrease in the partial molar free energy of mixing and thus with an increase in polymer–solvent interaction.

It should be noted that when polymer solutions in different solvents need to be compared, the use of relative rather than absolute viscosity allows taking into consideration the variation in viscosity of solvents. Consequently, the relative viscosity becomes a convenient measure of polymer–solvent interactions in polymer solutions of the same concentration.[33]

Table II summarizes some solvent-related properties including the relative viscosities of polymer solutions, which were used for casting of SPPO films, at 25°C. It can be noticed that the relative viscosities listed in the table vary from 10.09 for the pyridine solution to 21.89 for the tetrahydrofuran (THF) solution. Considering that polymer–solvent interactions decrease with an increase in the relative viscosity, these interactions increase in the following order: THF $<$ DMF $<$ DMAC $<$ NMP $<$ pyridine.

TABLE II
Solvent-Related Properties for 4.0 g/dL Solutions of High Molecular Weight SPPO

Solvent	M (g/mol)	V (cm^3/mol)	$T_{N.B.P.}$ (°C)	$T_{casting}$ (°C)	P_v (kPa)	η (cP)	η_{rel} (−)
NMP	99.13	96.5	202	60	0.45	1.593	10.27
DMAC	87.62	92.5	164.5	60	2.01	0.887	17.98
DMF	73.10	77.0	153	60	3.71	0.768	18.87
Pyridine	79.10	80.9	115	40	5.94	0.834	10.09
THF	72.11	81.7	65	25	22.0	0.453	21.89

M: molecular weight of solvent; V: molar volume; T_{NBP}: normal boiling point; $T_{casting}$: casting temperature; P_v: vapor pressure at casting temperature; η: dynamic viscosity; η_{rel}: relative viscosity.

Other solvent properties

Other parameters listed in Table II include environmental temperature during casting, normal boiling point of solvents, vapor pressure of solvents at the listed environmental temperatures, and the molar volume of solvents.

The importance of molar volume as a parameter determining the properties of solution-cast films arises from the fact that solvent molecules in casting solution might act as transient templates. As a result the films prepared using "large" solvents might have more free volume than those prepared using "small" solvents.[32] However, as shown in Table II the molar volumes of solvents utilized in this study are comparable. The smallest solvent–DMF and the largest solvent–NMP differ only by 25%. Moreover, the effect of molar volume was evident only above some critical molar volume, which in case of polysulfones was about 150 mL/mol.[32] Consequently; the effect of molar volume of solvent on properties of SPPO films considered in this study should be negligible.

The parameters such as environmental temperature during casting, normal boiling point and vapor pressure of solvent at environmental temperature relate to volatility of solvent in casting solution, which in turn influences desolvation and gelation kinetics in cast, wet films.[28] As a result, it is possible that these parameters influence the molecular structure and hence the properties of dry films. Unlike the molar volumes, the differences in volatility of solvents considered in this study are very significant. This is particularly evident when the vapor pressures listed in Table II are considered.

Thermogravimetric analysis

Themogravimetric analysis (TGA) is a convenient method to detect and quantify the concentration of residual solvent in polymeric films. If polymer contains residual solvent, the TGA spectrum will show a weight loss corresponding to the concentration of residual solvent. This weight loss, however, might not entirely occur around the temperature corresponding to the boiling point of solvent. This is because some residual solvent might be trapped in Langmuir sorption sites from which it can only be removed when Langmuir sorption sites cease to exit, that is, when the polymer undergoes the transition from the glassy to the rubbery state. Consequently, a TGA spectrum of a film containing residual solvent might show two separate weight loss regions, one around the boiling point of solvent and another one around the T_g of polymer.

Figure 2 shows the TGA spectra of SPPO films prepared from THF, DMF, and NMP solutions, respectively. For the clarity of picture, the spectra of pyridine and DMAC films are not shown. It can be noticed that regardless of solvent the spectra of SPPO films are similar to each other. In general, they show three weight loss stages followed by the final decomposition of polymer. As discussed elsewhere,[7,21] the first weight loss stage up to 100°C is due to the loss of water vapor absorbed by the films. The second weight loss stage, which occurs between 175 and 300°C, is due to decomposition of sulfonic groups, while the third weight loss stage, which occurs from 300 up to 400°C is related to the beginning of splitting of main chains before the final decomposition of polymer. The fact that the location of weight loss stages does not depend on the solvent in casting solution indicates that if there is any residual solvent in these films it exists only in Langmuir sorption sites. This is not surprising consid-

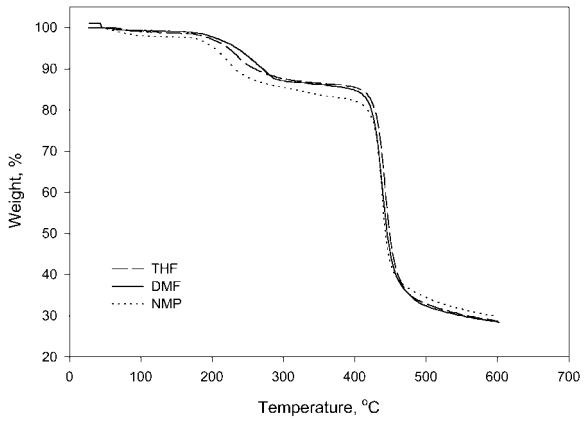

Figure 2 Thermal stability of dense SPPO films prepared from different casting solutions.

TABLE III
Summary of TGA Analysis of Dense SPPO Films Prepared from Different Casting Solutions

Solvent	Weight loss (wt %) First stage	Second stage	Third stage	Residual solvent (wt %)
NMP	2.5	11.0	4.8	4.8
DMAC	2.0	11.0	3.0	3.0
DMF	1.0	11.8	2.9	3.7
Pyridine	1.5	11.5	4.0	4.5
THF	2.0	10.8	3.6	3.4

ering the film drying protocol and the fact that TGA spectra were obtained on films previously tested for gas permeation.

In case of SPPO films shown in Figure 2, quantification of the concentration of residual solvent is difficult because of the weight loss due to decomposition of sulfonic groups. If the films indeed contained residual solvent in Langmuir sorption sites it would be a part of the second and perhaps the third weight loss stages in Figure 2. Consequently, the total weight loss in the second and third stages minus the mass fraction of sulfonic groups, which in the case of SPPO of DS equal to 18.5% is 11 wt %,[6] might give a rough estimation for the concentration of residual solvent in SPPO films considered.

Table III presents the summary of the TGA analyses for all SPPO films. Along with the weight losses in each stage, the table provides the estimated values for the concentration of residual solvent in each film. It can be noticed that depending on the solvent in casting solution, the concentration of residual solvent ranges from 3% in DMAC film to 4.8% in NMP film. Generally, the estimated concentrations of residual solvent is SPPO films are comparable to 4% of residual solvent reported in 6 FDA/mPDA polyimide films.[20]

In addition to estimation of the concentrations of residual solvent from TGA spectra, these concentrations were also estimated by comparing of the mass of films measured after being dried in vacuum for two days (before the coupons were cut and put into the testing cells, that is, before the final drying stage) with the theoretical mass of the films. The latter was calculated based on the concentration of polymer solution and the volume of polymer solution used for the film formation. According to this comparison, the films before the final drying stage contained 6.0–7.5% of residual solvent, regardless of the solvent used in casting solution. Although these concentrations are slightly greater than the concentrations listed in Table III, they indicate that the concentrations of residual solvent determined from the TGA spectra are reasonable.

Considering the properties of casting solutions listed in Table II, it is evident that the largest fraction of residual solvent is associated with the film prepared from the least volatile solvent—NMP. On the other hand, the second in this category is the film prepared from pyridine—the second most volatile solvent considered here. Interestingly, NMP and pyridine solutions show significantly lower relative viscosities compared to the other solutions. Considering the relationship between the polymer–solvent interactions and the relative viscosity, the larger concentrations of residual solvent in NMP and pyridine films might indicate that the concentration of residual solvent in polymeric films is primarily determined by the polymer–solvent interactions existing in the casting solution. This should not be surprising, since residual solvent in SPPO films is present in Langmuir sorption sites, and its concentration retained in these sites should increase as polymer–solvent interactions become stronger. On the other hand, volatility of solvent would be a dominant parameter determining the concentration of residual, if there were excess in amount that stays outside the Langmuir sorption sites.

Considering DMF, DMAC and THF films, the effect of polymer–solvent interactions discussed above does not seem to apply to the estimated concentrations of residual solvent in these films. It should be remembered, however, that the relative viscosities of respective polymer solutions did not vary significantly.

Comparison of surface morphologies

Atomic force microscopy has often been used for characterization of pore structure and surface morphology of polymeric membranes.[17,34–43] Although even the highest achievable resolutions of AFM are not sufficient to observe features, which directly control gas transport properties of polymeric films, the comparison of AFM images is thought to be useful in accessing the effect of solvent on surface morphology of polymeric films.

Figures 3–9 show samples of surface images of the films considered in this study. The images in Figures 3–7 are presented in a 12 × 12 μm scanning area with a 1.0 μm Z range, while the images in Figures 8 and 9 are presented in a 0.75 × 0.75 μm scanning area with a 50 nm Zrange. It should be emphasized that Zaxis in all images is expanded relative to the XYplane; there-

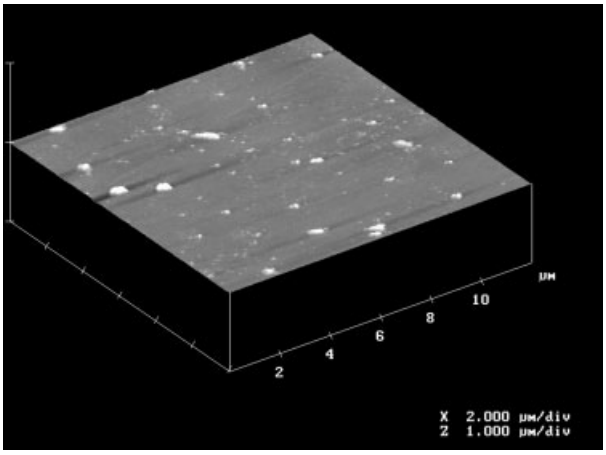

Figure 3 Surface image 12 × 12 μm scan size by AFM in tapping mode of dense SPPO film prepared from NMP solution.

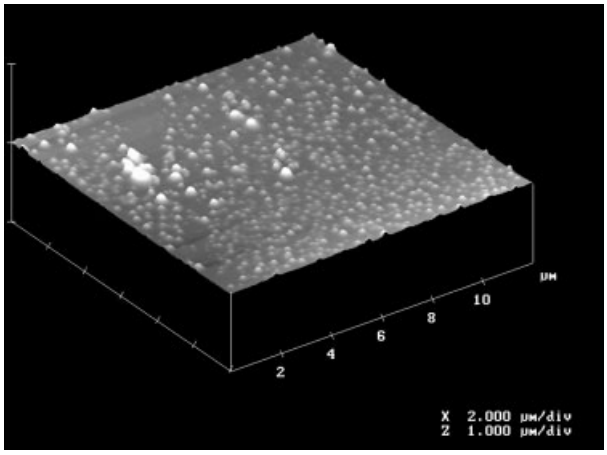

Figure 5 Surface image 12 × 12 μm scan size by AFM in tapping mode of dense SPPO film prepared from DMAC solution.

fore, the surfaces are not as "bumpy" as they appear on the images. The average values of roughness parameters for each type of film are summarized in Table IV.

The surface images of films prepared from NMP and pyridine solutions (Figs. 3 and 4) are not uniform. Some irregular features are found on a smooth background. These images are markedly different from those of films prepared from DMAC, DMF, and THF solutions (Figs. 5–7), which show relatively uniform granular structures. Quantitatively, irregularity of surface image can be expressed by the ratio of R_q/R_a parameters. Considering that R_a indicates the average Zvalue, while R_q the standard deviation from Zvalues; an increase in the R_q/R_a ratio should indicate more surface irregularity.[7] It is evident from Table IV that the R_q/R_a ratios for NMP and pyridine films are significantly greater than for the other films. At the same time, the roughness parameters R_a for NMP and pyridine films are several times less than for DMAC, DMF, and THF films.

On the surface of films prepared from NMP and pyridine bright spots of sizes ranging from 100 to 400 nm are observed (Figs. 3 and 4). According to Kesting,[32] these are macromolecular aggregates called nodular aggregates. These nodular aggregates cover larger area of the film surface as we progress from Figure 5 to Figure 7, while at the same time the size of nodular aggregates becomes larger. Especially in Figure 7, smaller grains start to emerge between larger grains. These smaller grains are believed to be macromolecular aggregates (nodules), according to Kesting's definition. An attempt to investigate these nodules in small scan size failed, because of poor resolution of the instrument. The problem of obtaining high-resolution images on rough surfaces was discussed elsewhere.[39]

Investigation of films prepared from NMP and pyridine in a small scan size was, on the other hand,

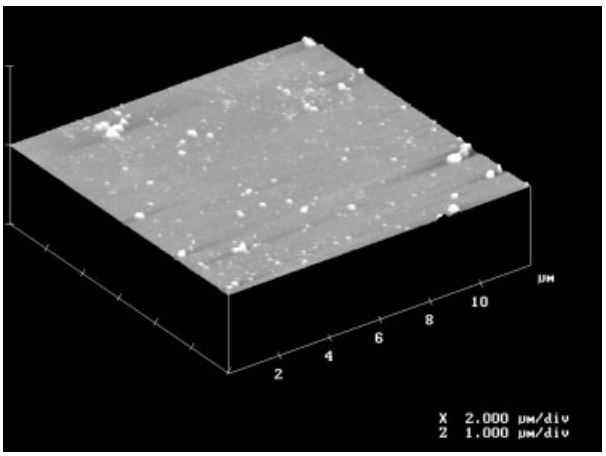

Figure 4 Surface image 12 × 12 μm scan size by AFM in tapping mode of dense SPPO film prepared from pyridine solution.

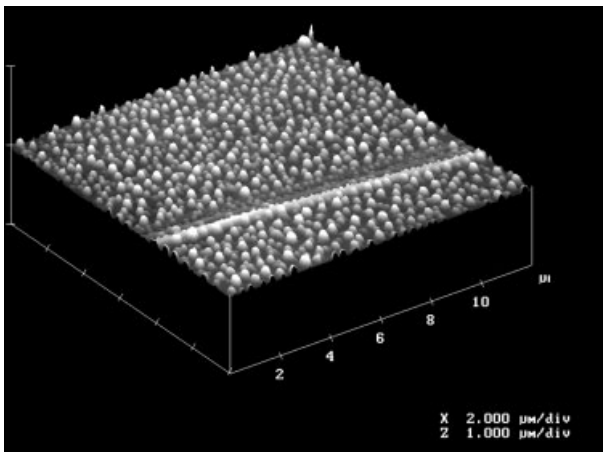

Figure 6 Surface image 12 × 12 μm scan size by AFM in tapping mode of dense SPPO film prepared from DMF solution.

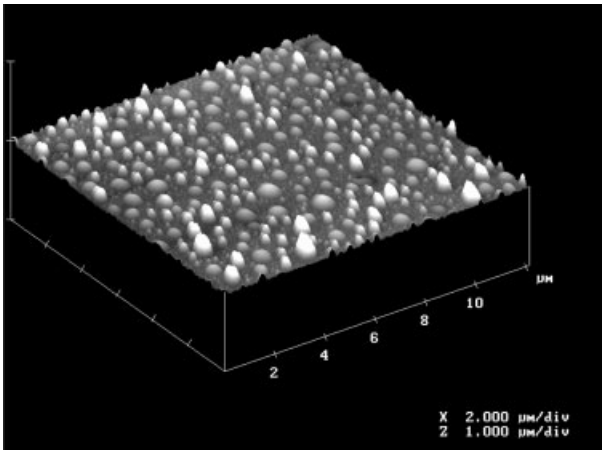

Figure 7 Surface image 12 × 12 μm scan size by AFM in tapping mode of dense SPPO film prepared from THF solution.

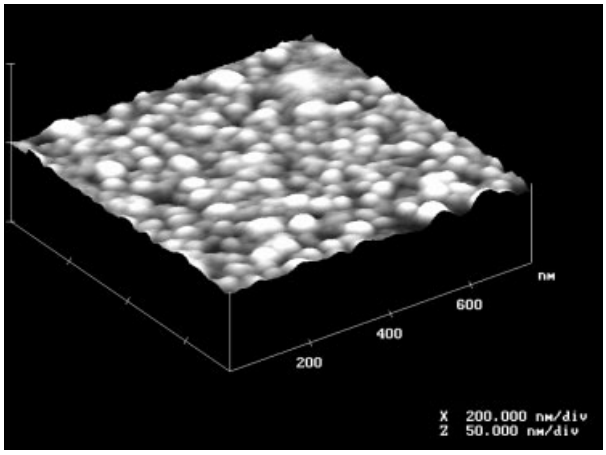

Figure 9 Surface image in 0.75 × 0.75 μm scan size by AFM in tapping mode of dense SPPO film prepared from pyridine solution.

possible. The grain sizes observed on Figures 8 and 9 range from 30 to 60 nm, corresponding to those of nodules.

The differences in surface morphology between films prepared using different solvents in casting solutions are undeniable, especially when NMP and pyridine films are compared with DMAC, DMF, and THF films. The formation of large nodular aggregates, evident on surface images of the latter films, should be favored by strong polymer–polymer interactions. In this study however, since all films were prepared from the same polymer these interactions should be the same. On the other hand, the forces responsible for aggregation of macromolecules—the dispersive, polar, and hydrogen-bonding forces are generally short-range forces, and consequently solvent molecules entrapped between polymer chains might significantly attenuate them, leading to some differences between films prepared form different solutions. Interestingly,

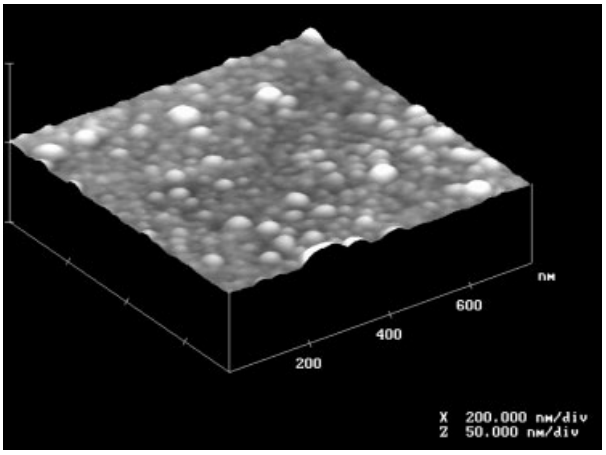

Figure 8 Surface image in 0.75 × 0.75 μm scan size by AFM in tapping mode of dense SPPO film prepared from NMP solution.

the films with the largest concentration of residual solvent–NMP and pyridine have the "smoothest" surface images, which would suggest a direct link between the concentration of residual solvent and surface morphology.

On the other hand, considering the link between concentration of residual solvent and polymer–solvent interactions, the differences in surface morphologies could also be related to the properties of solvent in casting solution—in particular, to the strength of polymer solvent interactions. It should be noted that the strength of polymer solvent interactions decreases in the order NMP ≈ pyridine > DMAC > DMF > THF, according to the relative viscosity data given in Table II. This is exactly the same as the order in morphology change from Figure 3 to Figure 7, where the size of nodular aggregates increases progressively, which suggests a direct correlation between morphology and polymer solvent interactions.

In the case of comparable polymer–solvent interactions, surface roughness appears to increase with volatility of casting solution. This is evident when NMP and pyridine films are compared with each other and when similar comparison is made between DMAC, DMF, and THF films. The effect of volatility of solvent

TABLE IV
Summary of Surface Roughness Parameters for Dense SPPO Films Prepared from Different Casting Solutions

Solvent	Number of images	Scan size μm × μm	R_a (nm)	R_q (nm)	R_q/R_a (−)
NMP	4	12 × 12	1.53	3.13	2.04
Pyridine	4	12 × 12	2.30	4.56	1.98
DMAC	6	12 × 12	12.5	16.8	1.34
DMF	4	12 × 12	22.3	28.9	1.30
THF	4	12 × 12	34.8	44.9	1.29
NMP	1	0.75 × 0.75	0.69	0.98	1.42
Pyridine	1	0.75 × 0.75	1.06	1.37	1.29

TABLE V
Summary of Gas Permeation Properties of Dense High Molecular Weight SPPO Films Prepared from Different Casting Solutions

	Permeability (barrer)				Permeability ratio	
Solvent	N_2	O_2	CH_4	CO_2	O_2/N_2	CO_2/CH_4
NMP	0.25	1.74	0.20	7.54	6.95	38.39
	0.27	1.86	0.22	8.63	6.88	39.22
Pyridine	0.77	4.69	0.68	23.51	6.09	34.65
	0.83	5.03	0.77	26.27	6.06	34.12
DMF	0.44	2.74	0.36	13.10	6.24	36.72
	0.51	3.25	0.42	15.09	6.38	35.94
DMAC	0.45	2.85	0.34	13.15	6.29	37.10
	0.54	3.38	0.45	16.29	6.30	36.28
	0.51	3.24	0.46	16.04	6.40	34.81
THF[a]	0.56	3.59	0.53	17.37	6.36	32.97
	0.66	4.07	0.62	21.02	6.16	33.91
	0.62	3.86	0.54	17.68	6.26	32.96

[a] All THF films were laminated with silicone rubber films; permeability of defective films was estimated using Eq. 2.

in the casting solution on surface morphology of polymeric films observed in this study is consistent with earlier reports.[17,41,42]

Gas transport properties

The discussed differences in surface morphologies relate to the tendency to form macromolecular aggregates as well to the size of these aggregates. The question that arises is, Do these differences correlate in any way to gas transport properties of polymeric films? Table V presents the summary of permeabilities and permeability ratios of SPPO films prepared from different casting solutions. It is evident from the table that gas transport properties change with solvent in casting solution. For example, by changing the solvent in casting solution from NMP to pyridine, the O_2 and CO_2 permeabilities of SPPO increase by more than three times. This increase is associated with a 10–15% decrease in O_2/N_2 and CO_2/CH_4 permeability ratios. Although the variation in gas transport properties of SPPO films is quite significant, it is still relatively small in comparison with a sixfold increase in permeability of dense poly(4-methyl-1-pentane) resulting from the change of casting solvent from chloroform to cyclopentane.[16]

Interestingly, the most permeable (pyridine) and the least permeable (NMP) films are those having similar surface morphologies. This suggests that there is no direct link between the level of surface structure observed by AFM and gas transport properties of SPPO films. Moreover, NMP and pyridine are the strongest solvents for SPPO among the solvents considered. Consequently, permeability of solution-cast SPPO films cannot be directly related to polymer–solvent interactions existing in casting solution. The NMP and pyridine films are also those that contained the largest concentration of residual solvent. Considering that residual solvent occupies the Langmuir sorption sites, which would otherwise be available for the permeating gas, these two films should be the least permeable for gases.[28] Comparing permeabilities and permeability ratios with the concentration of residual solvent, it becomes evident that there is no direct correlation between the gas transport properties and the concentration of residual solvent. While this might indicate that for the reported range of concentrations of residual solvent, its presence does not influence the gas transport properties of SPPO films, it should also be emphasized that the reported concentrations of residual solvent are only rough estimates. Moreover, the differences in concentration of residual solvent from film to film (3.0–4.8%) are relatively small.

On the other hand, the lack of a direct correlation between gas transport properties and concentration of residual solvent might indicate that the effect of residual solvent on gas transport properties is more complicated than a simple proportionality relationship. The SPPO, because of the presence of active —SO_3H groups, can be considered as a weak acid capable of reacting with solvents containing strong nucleophilic groups. Considering the solvents used in this project, their nucleophilicity (basicity) increases in the following order: THF $<$ DMAC $\approx$ DMF $\approx$ NMP $<$ pyridine. Consequently, it is possible that films prepared from the pyridine solution contained quaternary salts formed between a proton from the sulfonic group of SPPO and the pyridine's nitrogen. It is important to emphasize, however, that although pyridine is the only solvent used in this project, which could be considered as a base, it is still a very weak base. Moreover, as already mentioned in the Experimental section, to facilitate the removal of films from the casting plate, they were immersed in distilled water, which could result in hydrolysis of any existing quaternary salts. However, the significant difference in gas transport properties between the films prepared from pyridine and NMP solutions might indicate the pyridine films contained quaternary salts, which made them chemically different the NMP and any other films studied in this project.

Alternatively, the outstanding gas transport properties of pyridine films can be explained on the basis of different volatility of solvent in different casting solutions. According to Khulbe et al.,[17] an increase in solvent volatility results in preserving more of the polymer structure present in the polymer solution. Consequently, films prepared from more volatile solvents will have more random structures, greater free volumes, and greater permeabilities for gases than those prepared from the less volatile solvents. This argument could be used to explain greater permeabilities of pyridine compared to NMP films, since pyri-

dine volatility is higher than NMP volatility, while polymer–solvent interactions are nearly equal. Moreover, remembering that nonlaminated THF films had very high permeability and no selectivity, the comparison of volatilities listed in Table II with permeabilities listed in Table V reveals that with the exception of DMAC films, which are slightly more permeable than DMF films, permeability increases with volatility of solvent in casting solution.

The question that arises is, Why of all films only those made from THF solution were defective? It is evident from Table II that THF is significantly more volatile than the other solvents. On the other hand, there are solvents, even more volatile than THF, for example chloroform, which yield defect-free polymeric films. Therefore, the defective structure of THF films cannot be attributed only to high volatility of this solvent. Interestingly, THF is not only the most volatile but also the weakest solvent for SPPO among the studied solvents. Weak polymer–solvent interactions enhance formation of macromolecular aggregates in THF solution. The excessive growth of macromolecular aggregates together with rapid evaporation of solvent will lead to incomplete coalescence of these aggregates and consequently to defects in the film structure. It is therefore postulated that combination of weak polymer–solvent interactions and high volatility of casting solution should be avoided in order to prevent formation of defects in polymeric films.

Figure 10 shows the performance of SPPO films with respect to an upper bound line for O_2/N_2 and CO_2/CH_4 separations.[44] The points in Figure 10 represent the average permeabilities and permeability ratios from Table V. It can be noticed that despite significant differences in O_2 and CO_2 permeabilities, the distance from the upper bound line is similar for the films prepared from different casting solutions. This is because an increase in permeability is associated with a decrease in selectivity, which is a typical trade-off behavior of polymeric membranes.[44]

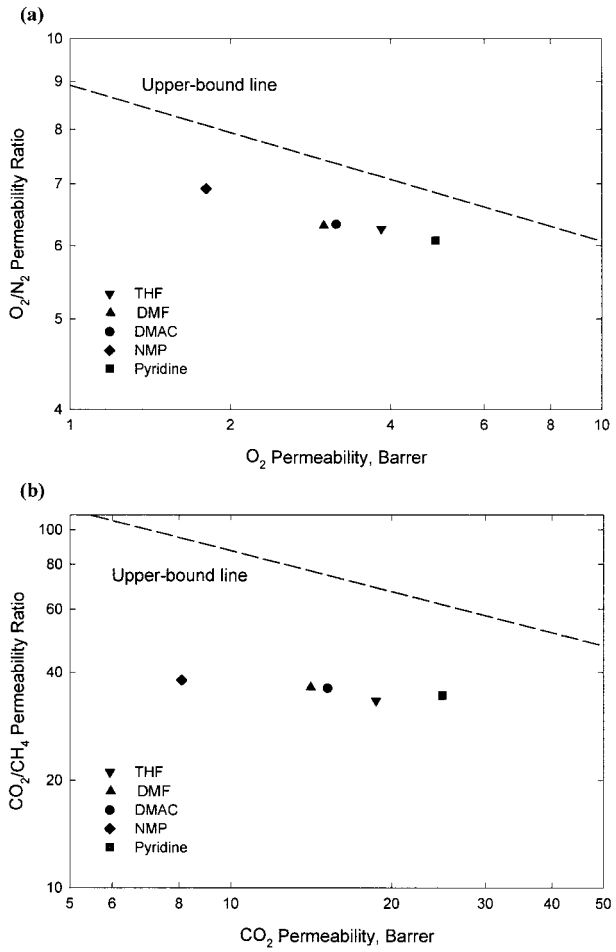

Figure 10 Effect of solvent in casting solution on combination of (a) O_2 permeability and O_2/N_2 permeability ratio, and (b) CO_2 permeability vs. CO_2/CH_4 permeability ratio of dense high molecular weight SPPO films.

CONCLUSION

Change of solvent in casting solution inevitably leads to simultaneous changes in polymer–solvent interactions, molar volume, and volatility of casting solution. The current study involving SPPO and five different solvents having relatively similar molar volumes revealed that polymer–solvent interactions expressed by the relative viscosity of casting solution primarily determine the concentration of residual solvent and the surface morphology of solution-cast dense SPPO films. In particular, the increasing surface roughness of dense films with an increase in the relative viscosity of casting solution is clearly evident. On the other hand, permeability of SPPO films, which increases by more than three times when NMP is replaced by pyridine as a solvent in casting solution, appears to be governed by volatility rather than polymer–solvent interactions. In addition, it is possible that the outstanding gas transport properties of the films prepared from the pyridine solution could result from the existence in these films of quaternary salts formed between sulfonic groups and pyridine's nitrogen.

The current study did not reveal a direct correlation between the surface morphology observed at a given resolution of AFM equipment and the gas transport properties of solution-cast dense SPPO films. The analysis of surface images by AFM, however, allowed pinpointing unfavorable surface morphology resulting from a particular combination of casting solution properties. Essentially, the combination of high volatility and weak polymer–solvent interactions in THF solution resulted in a very high surface roughness of the resulting films, which lead to some structural defects manifested by very high permeability and no selectivity for gases of these films.

The authors gratefully acknowledge the financial support of the Natural Sciences and Engineering Research Council of Canada and British (Consumers) Gas. The authors also would like to express their gratitude to Dr. Z. Y. Wang and his student Mr. T. Bender for the thermogravimetric analysis of the films.

References

1. Ward, W. J., III; Salemme, R. M. U.S. Pat. 3,780,496, 1973.
2. Percec, S.; Li, G. ACS Symp Ser 364, 16, 1988.
3. Bikson, B.; Gotz, G.; Ozcauir, Y.; Nelson, J. K. U.S, Pat. 5,348, 569, 1994.
4. Fu, H.; Jia, L.; Xu, J. J Appl Polym Sci 1994, 51, 1405.
5. Polotskaya, G. A.; Agranova, S. A.; Antonova, T. A.; Elyashevich, G. K. J Appl Polym Sci 1997, 66, 1439.
6. Kruczek, B.; Matsuura, T. J Membrane Sci 1998, 146, 263.
7. Kruczek, B. Ph.D. thesis, University of Ottawa, Ottawa, ON, 1999.
8. Kruczek, B.; Matsuura, T. J Membrane Sci 2000, 167, 203.
9. Jones, G.; Miles, J. J Soc Chem Ind 1933, 52, T251.
10. Hass, H.; Farney, L.; Valle, C., Jr. J Colloid Sci 1952, 7, 584.
11. Doolitle, A. K. The Technology of Solvents and Plasticizers; John Wiley: New York, 1954.
12. Katz, R.; Munk, B. J Oil Colour Chemists' Assoc 1969, 52(5), 418.
13. Pacter, A.; Nerurkar, M. Eur Polym J 1968, 4(6), 685.
14. Zubov, P.; Voronkov, V.; Sukhareva, L. Chem Abstr 1968, 68, 96306g.
15. Okuno, H.; Renzo, K.; Uragami, T. J Membrane Sci 1993, 83, 199.
16. Mohr, J. M.; Paul, D. R. Polymer 1991, 32, 1236.
17. Khulbe, K. C.; Kruczek, B.; Chowdhury, G.; Gagne, S.; Matsuura, T. J Appl Polym Sci 1996, 59, 1151.
18. Maeda, Y.; Paul, D. R. J Membrane Sci 1987, 30, 1.
19. Moe, M.; Koros, W. J.; Hoehn, H. H.; Husk, G. R. J Appl Polym Sci 1988, 36, 1833.
20. Joly, C.; Le Cerf, D.; Sauvage, J. P.; Chappey, C.; Langevin, D.; Muller, G. STEPI 4, 1996, 379.
21. Fu, H.; Jia, L.; Xu, J. J Appl Polym Sci 1994, 51, 1399.
22. Plummer, C. W.; Kimura, G.; LaConti, A. B. Office of Saline Water Research and Development Progress Report No. 551, General Electric Co., Lynn, MA, 1970.
23. Huang, R. Y. M.; Kim, J. J. J Appl Polym Sci 1984, 29, 4017.
24. Hansen, C. M.; Beerbower, A. In Solubility Parameters in Kirk-Othmer Encyclopedia of Chemical Technology, 2nd ed.; Standen, A., Ed.; Interscience: New York, 1971; Suppl Vol 889.
25. Kruczek, B.; Matsuura, T. J Membrane Sci 2000, 177, 129.
26. Henis, J. M. S.; Tripodi, M. K. J Membrane Sci 1981, 8, 233.
27. Digital Instruments, Inc. NanoScope III, Control System Manual; Santa Barbara, CA, December 1993.
28. Kesting, R. E.; Fritzsche, A. K. Polymeric Gas Separation Membranes; John Wiley & Sons: New York, 1993.
29. Barton, A. F. M. CRC Handbook of Solubility Parameters and Other Cohesion Parameter; CRC Press: Boca Raton, Fl, 1983; Chap 15.
30. Ferry, J. D.; Foster, E. L.; Browning, G. V.; Sawyer, W. M. J Colloid Sci 1951, 6, 377.
31. Gandhi, K. S.; Williams, M. C. J Polym Sci C 1971, 35, 211.
32. Kesting, R. E. J Appl Polym Sci 1990, 41, 2739.
33. Hoernschemeyer, D. H. J Appl Polym Sci 1974, 18, 61.
34. Kesting, R. E.; Fritzsche, A. K.; Handermann, A. C.; Murphy, M. K.; Cruse, C. A.; Malon, R. F.; Moore, M. D. J Appl Polym Sci 1990, 40, 1557.
35. Fritzsche, A. K.; Arevalo, A. R.; Moore, M. D.; Elings, V. B.; Kjoller, K.; Wu, C. M. J Membrane Sci 1992, 68, 65.
36. Fritzsche, A. K.; Arevalo, A. R.; Moore, M. D.; Weber, C. J.; Elings, V. B.; Kjoller, K.; Wu, C. M. J Appl Polym Sci 1992, 46, 167.
37. Fritzsche, A. K.; Arevalo, A. R.; Connoly, A. F.; Moore, M. D.; Elings, V. B.; Wu, C. M. J Appl Polym Sci 1992, 45, 1945.
38. Dietz, P.; Hansma, P. K.; Inacker, O.; Lehmann, H. D.; Herrmann, K. H. J Membrane Sci 1992, 65, 101.
39. Bowen, W. R.; Hilal, N.; Lovitt, R. W.; Williams, P. M. J Membrane Sci 1996, 110, 229.
40. Bowen, W. R.; Hilal, N.; Lovitt, R. W.; Williams, P. M. J Membrane Sci 1996, 110, 233.
41. Khulbe, K. C.; Kruczek, B.; Chowdhury, G.; Gagne, S.; Matsuura, T.; Verma, S. P. J Membrane Sci 1996, 111, 57.
42. Khulbe, K. C.; Chowdhury, G.; Kruczek, B.; Vujosevic, R.; Matsuura, T.; Lamarche, G. J Membrane Sci 1997, 126, 115.
43. White, L. S.; Blinka, T. A.; Kloczewski, J.; Wang, I. J Membrane Sci 1995, 103, 73.
44. Robeson, L. M. J Membrane Sci 1991, 62, 165.